Rohaan Deb, Niraj Kakoty
Group P24

Advanced Lab Course: Nuclear γ-γ angular correlations (K223)

February 20, 2020
Tutor: Christian Honisch
Universität Bonn

Contents

1 Introduction

Radioactive sources emit electromagnetic radiation in a isotropic way which is because the atomic nuclei are isotropic. But, if intermediate m-levels of an excited nucleus are not equally occupied, the emitted radiation is anisotropic. An excited nucleus formed after Beta or Alpha decay subsequently goes to the stable state by emitting gamma rays. In this γ-γ cascade, an orientation of spins can be achieved if we measure the direction of flight of the first γ-quant and define this direction as the quantisation axis. This results in an anisotropic angular distribution for the second γ-quant. This angular correlation between the two γ rays is given by a multipole expansion, the coefficients of which can be used to determine important properties of the nucleus like the momentum distribution, spin of intermediate state, internal fields of the nucleus.
The aim of our experiment is to measure the γ-γ angular correlaton in the decay of ^{60}Co by determining the multipole expansion coefficients experimentally and compare them against the theoretically obtained values.

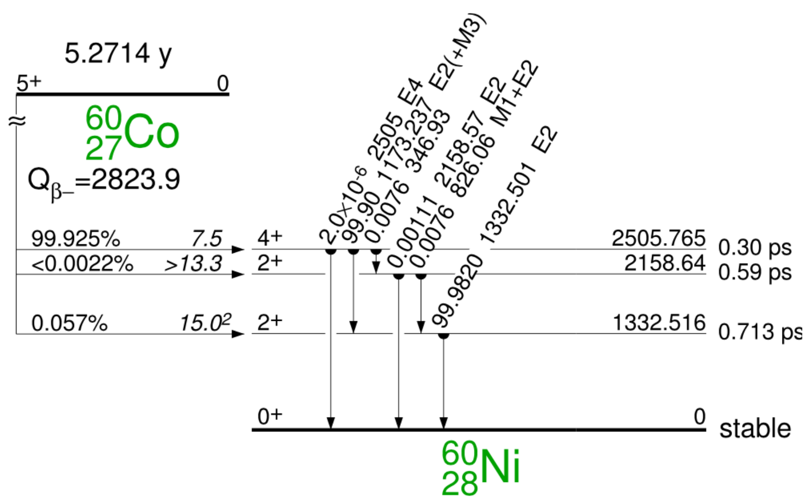

Figure 1: Decay scheme of ^{60}Co (Source[2])

2 Theoretical Principles

The ^{60}Co isotope undergoes β-decay with a half-life of 5.272 years.

$$^{60}Co \rightarrow {}^{60}Ni{+}e^{-}{+}\bar{\nu_e}$$

The decay is initially to an intermediate state of Ni-60 from which it can emit a cascade of γ-rays to reach ground state. Due to this intermediate state, the spins of the state can couple to with the angular momenta of the emitted photons and the successive gamma rays have a anisotropic emission. This angular correlation of the two gamma rays can be studied in a cascade.
The ^{60}Ni relaxes by the emission of 2γ-rays of energy 1.17 MeV and 1.32 MeV, via the most probable decay scheme(Figure 1) $4^{+}{\rightarrow}2^{+}{\rightarrow}0^{+}$. The probability of this decay to occur is 99% and the short half-life of ^{60}Co, makes it a perfect candidate for this experiment.
In the absence of any external perturbations, the **Angular Correlation** function, which is defined as the relative probability of the second γ-quant being emitted at an angle θ with respect to the first one, is given as-

$$\mathrm{W}(\theta){=}1{+}A_{22}cos^{2}\theta + A_{44}cos^{4}\theta$$

where A_{22} and A_{44} are the angular correlation coefficients. Theoretically, the coefficients were found out to be-

$$A_{22} = 0.125, A_{44} = 0.042$$

or,

$$\mathrm{W}(\theta){=}1{+}0.125cos^{2}\theta + 0.042cos^{4}\theta$$

3 Apparatus

3.1 Detection

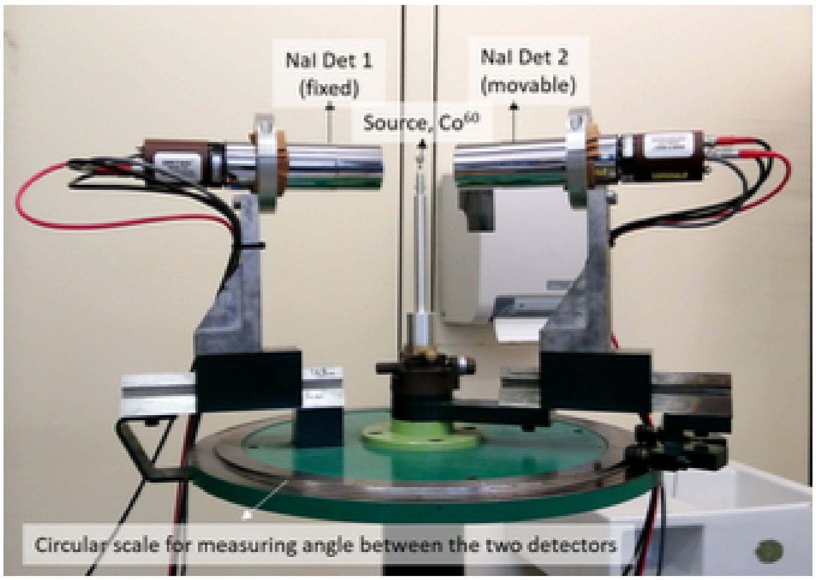

Figure 2: Detector and source setup

The detecting mechanism consists of two NaI(Tl) cylindrical scintillators of dimensions 2”diameter x 2”long with photo-multipliers(PMTs) attached. The detectors are placed around the source such that one detector is fixed and the other is movable. Here, the photons can undergo either of the three interaction process, namely photo-effect, Compton effect or pair production. At low energies, Compton scattering is dominant, where the photons elastically scatter off electrons in the constituents of the crystal. The scattered photons, in this case would give a Compton spectrum at the output of the detector. At intermediate energies, the photons are completely absorbed by the material, and photo-electrons are ejected. These high energy electrons interact with the lattice as they pass through, creating a cascade of secondary, tertiary and so on, electrons and photons. The flux of these particles at the output of the scintillation detector is proportional to the energy of the primary photon. Similar process happens with pair production at very high energies (E$\geq 2m_e^2$), with an addition of electron-positron annihilation which gives out secondary photons. This detection method will have a very low effciency due to the two level nature of NaI crystal. In a two-level system, the photons in resonance will undergo absorption and re-emission multiple times, which can change the energy. To avoid this, NaI crystal is doped with Tl to convert the system into a three-level system, where the re-emission happens with 2 photons of lower energy. The

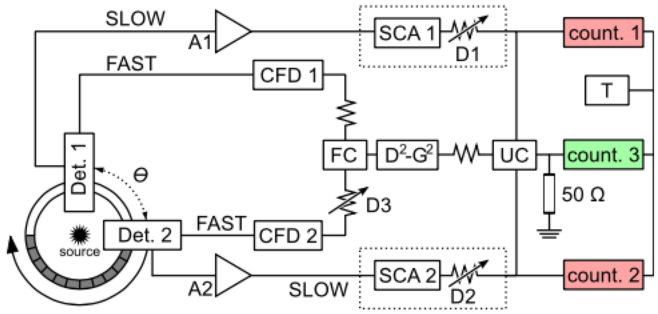

Figure 3: Schematics of the final setup used for the coincidence measurement. Detector 1 is fixed and Detector 2 allows rotation at a fixed radial distance from the source. The detectors are attached to FAST and SLOW coincidence circuits. Counters 1 and 2 counts the total decays measured in the Detectors 1 and 2 respectively, and Counter 3 counts the total coincidence decays. [source: Lab manual, K223: Nuclear γ-γ Angular Correlation [1]

crystal is more transparent for these photons, and hence the effciency of detection increases..
The output signal of the scintillators is proportional to the energy of the input photon. The photocathode in the PMT converts the output photons to electrons which are amplified by the dynodes in the PMT. Two signals are derived from each detector: a fast timing signal and the slow energy pulse.

3.2 Amplifiers

Multiple amplifiers were used at the output of the PMTs to increase the strength of the signals for further processing. One amplifier was used before the SCAs. The gain of the amplifiers were set to an optimum level such that the SCAs work linearly in the range 0-9V and signal amplification is maximum without any clip-off.

3.3 Single Channel Analysers

SCAs[5] were used to measure the energy of the photons and to set a criteria for selection of events to filter out the background and noise. This was done by using the window mode in the SCA and setting appropriate window widths such that only photons of specific energy range can be selected.

3.4 Constant Fraction Discriminator(CFD)

The CFD times the two γ-ray photons. The CFD[4] works as follows:

- Input Pulse is split into two parts
- One part is attenuated using a delay and applied to the inverting input of a discriminator
- The other part is applied to the non-inverting input of the same discriminator.
- These two signals are then added back together
- The zero point of the signal gives us timing information of the event.

In general, an analogue pulse is timed by a leading edge detection or a trailing edge detection method. In this method, the half maxima of the leading and trailing edge is measured.Since, γ-rays photons can have different energies and thus different pulse heights, they can have delays based on the pulse heights. A special property of the Scintillator-PMT signal is that the leading edge profile will always be the same. Thus, using the above mentioned method, we can measure the timing of the pulse, giving timing information regardless of the pulse height.

3.5 Fast Coincidence(FC)

The output of the two CFDs goes into the FC[6]. With a resolving time τ, if the signal from the CFDs lie within the window, the FC gives an output. Otherwise it does not give any output signal.The timescales of the nuclear decay are in the order of ps ($\approx 10^{-12}s$). Since most electronics work in a timescale of much larger order ($\approx 10^{-8}s$), one considers a γ-γ cascade to be simultaneous for the electronic detectors. Hence, setting the appropriate resolving time is important because it will help to filter out unwanted decays to 2γ photons.

3.6 Delays(D)

It has been found that two same components of any electronic system will have different delays and in order to compensate for this between different channels, delays are introduced such that the signals reach the respective parts at the same time.
For fast circuit, the dalays are caused by cables of different lengths. while for slow circuit, it is embedded within the SCA, the gate and the delay generator

3.7 Gate-Delay(G^2-D^2)

Similar to the delays, it compensates for the signal delay between the slow and fast branches of the circuit.

3.8 Universal Coincidence(UC)

The inputs from the fast and slow branches enter into the UC[7]. The UC will give an output only if outputs from G^2-D^2 and the two SCAs are simultaneous. Thus, the UC has a high output only when there has been a simultaneous measurement of 2γ photons in both the detectors within the set time frame τ, and the required energy range. The output of the UC implies that the required detection has occurred and is counted with electronic counter.

4 Exercises

4.1 Which distances to choose?

1. How does count rate of one detector change with distance?
   Answer: The count rate of a detector varies as follows

   $$\text{Count rate} \propto \frac{1}{r^2}$$

   where, r is the distance between the detector and the source.

2. How does the coincidence rate change with distance?
   Answer: The coincidence rate is also inversely proportional to the distance between the detector and the source.

   $$\text{Coincidence rate} \propto \frac{1}{r^4}$$

3. How does the asymmetry seen in the experiment differ from the theoretical prediction?
   Answer: An asymmetry has been found due to the fact that there can be misalignment of the source and depending on the position of the source the count rate varies.

4. How do the correction factors influence the error of the corrected correlation coefficients?
   Answer: Correction factors lead to an increase in the error of the calculated correlation coefficients.
   The larger the correction factor is, the smaller the measurable asymmetry will be. Hence, for a given statistical precision the more the correction is the more will be the error in calculation of correlation factors.

5. Using the values provided in Seigbahn for 1.5"$\times$ 1" crystals: which distance is likely to yield most precise results?
   Answer: For 7cm and 10 cm, the count rate will be small. Hence, 5cm is believed to be the ideal distance.

4.2 Which angles to pick?

1. Express the angular correlation using the coefficients A,α and β.
   Answer: The relation is as follows:

$$W(\theta) = A(1 + (\frac{\alpha+\beta}{2})cos^2\theta + (\frac{\alpha-\beta}{2})cos^4\theta)$$
$$= A(1 + \frac{\alpha}{2}(cos^2\theta + \cos^4\theta) + \frac{\beta}{2}(cos^2\theta - cos^4\theta))$$

2. Plot the function using the predicted values for C and B and slightly vary them. Use A=1.

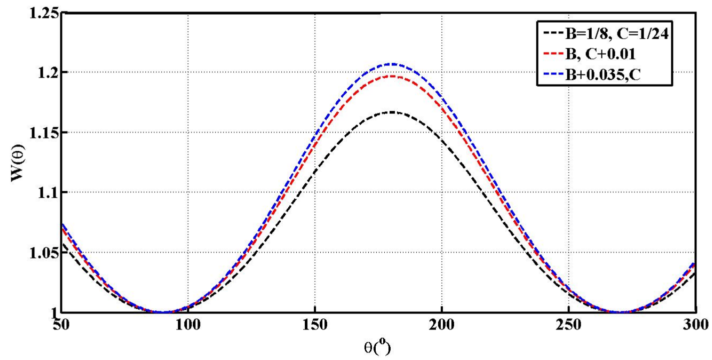

Figure 4: Theoretical predictions for angular correlation with A=1,B=$\frac{1}{8}$ and C=$\frac{1}{24}$ and slight variation in B and C

3. Plot the function for predicted values for α and β and plot them again but with a slightly varied α and once with slightly varied β.

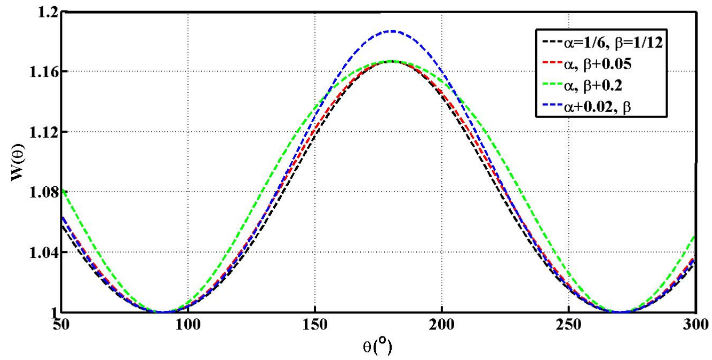

Figure 5: Theoretical prediction for angular correlation with A=1, $\alpha = \frac{1}{6}$ and $\beta = \frac{1}{12}$ and slight variation in α and β

4. How does the function change? At which points the largest change is observed?
Answer: It has been observed that varying α results in change in the amplitude of W(θ), as evident from the Fig.5. On the other hand, varying β slightly, the width of the curves changed while there is no alterations in the extrema of the curves. However, it is to be noted that small change in β does not effect the shape of the curve to a large extent.hence we can conclude that, the parameter, α changes the amplitude of the angular correlation function, while the parameter β changes the shape (width) of the same.

4.3 How to measure for de-adjustments?

1. How will the misalignment manifest in the data? How can you correct it?
Answer: Misalignment in data will manifest as an asymmetry in the angular correlation. The source must be placed at equal distances from both the detectors as possible initially to reduce this effect. This effect cannot be corrected completely, but one can reduce its effect by taking more values from 90 to 270 and using more values in curve fit.
It can be seen in both, the count rate of the mobile detector and the coincidence count rate that there is always some residual misalignment left. So we use the movable detector's count rate to compensate the impact on W(θ). Hence we plot the following graph which has angles as its abscissa and the ratio of coincidence count rate and movable count rate as the ordinate and compare it with that of the ratio of coincidence count rate and fixed count rate. The difference in the amplitudes suggest that in our experiment the movable detector was closer to the source that that of the fixed one. So, the misalignment is evident in our experiment. The formulas for count rate are also mentioned below.

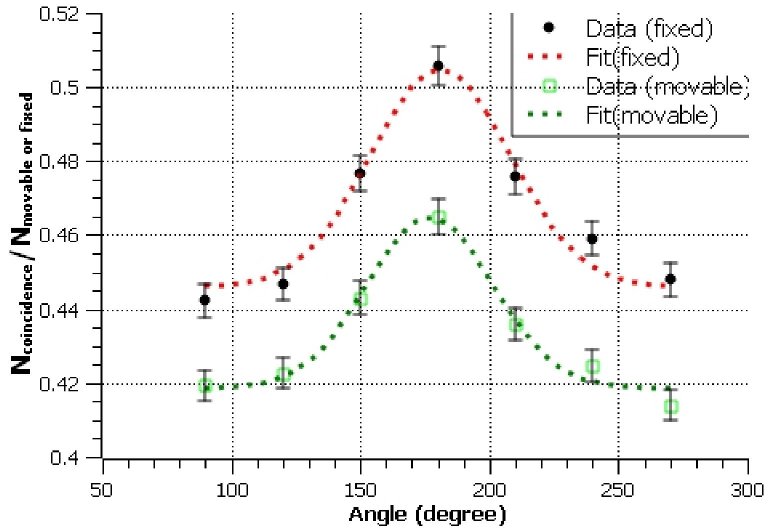

Figure 6: Ratio of $N_{coincidence}/N_{C2}$(movable counter) and $N_{coincidence}/N_{C1}$(fixed counter) plotted against the angles from 90°to 270°with a stepping of 30°.

Count Rate: The count rate for the fixed and movable counter can be given as-

$$N_i = n\epsilon_i \frac{\Omega_i}{4\pi}$$

where,
i= 1 for the fixed counter, 2 for the movable counter
n=number of γ rays per second emitted by an isotropic source.
ϵ= efficiency
Ω= solid angle

Thus, the coincidence rate can be written as-

$$\begin{aligned} N_{coincidence} &= N_1 N_2 \\ &= n\epsilon_1\epsilon_2 \frac{\Omega_1}{4\pi}\frac{\Omega_2}{4\pi} \end{aligned}$$

In general we can write,

$$f_{fix} = f_{movable} \sim \Omega A, and$$

$$f_{coincidence} \sim \Omega^2 A$$

(since B=C=0 and f(θ) = A)

5 Procedure

5.1 Preparation of setup

5.1.1 Preliminary Alignments

- The source was carefully placed on the mount at the center of the table.
- Alignment and orientation of the detectors was checked with the distance from the center being 5cm.
- The necessary connections were checked.

5.1.2 Energy Branch-Adjusting gain

Using an oscilloscope the outputs of the two amplifiers A1 and A2 were measured and set such that they were in the linear range. Both the outputs were at 7.2V. The range of the amplifier was from 0-9V and hence the outputs were in the linear range, as required.

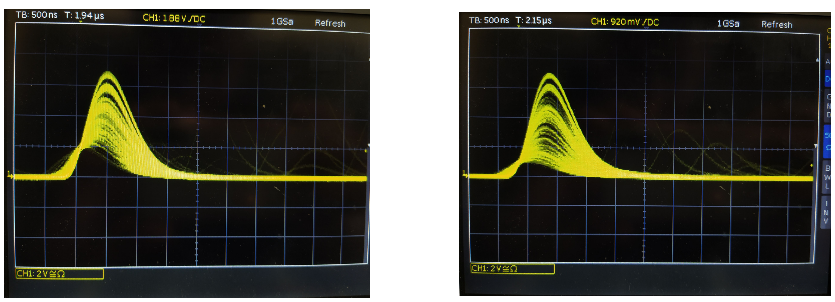

(a) Amplifier 1 (b) Amplifier 2

Figure 7: Adjusting gain of amplifiers

5.1.3 Timing Branch-Adjustment of CFD

The threshold had to be set such that maximum noise could be filtered out while not destroying the signal. A set of reading were taken by varying the thresholds of the CFDs, once with source and once without source. The counts was measured, which would tell us where signal/noise ratio is high. From the graphs, the threshold was set at 50mV for both. The lines joining the data points are to guide the eye and are no fit, interpolation, or prediction of any sort.

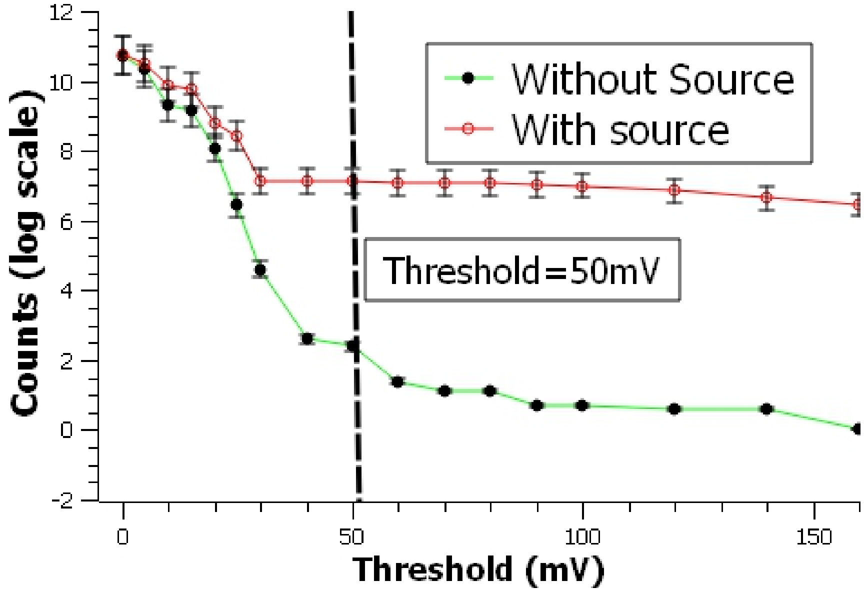

(a) CFD 1

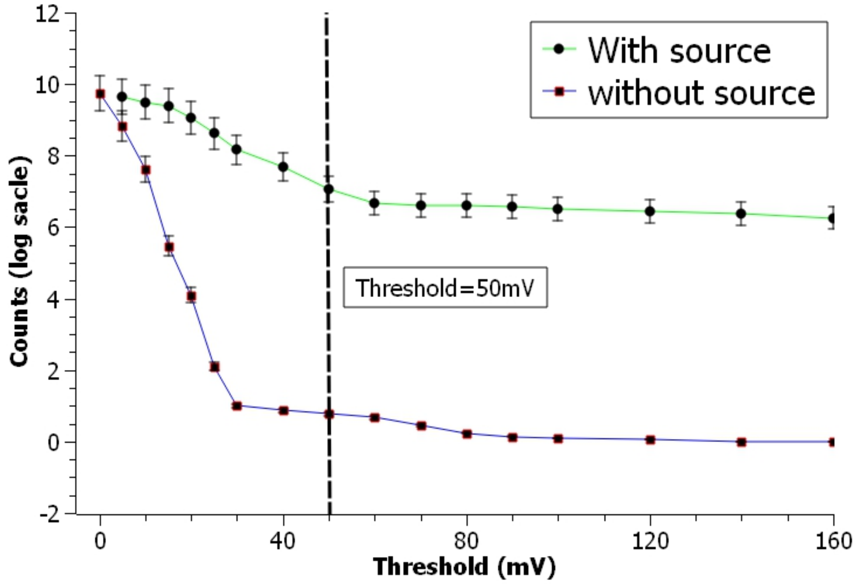

(b) CFD 2

Figure 8: Counts measured with and without source by varying CFD threshold

5.1.4 Setting up the fast coincidence

To compensate for the delay between the two fast signals, a fixed delay was introduced between a CFD and FC, and a variable in the other. The resolving time was set at τ=20ns and the output was connected to a counter through an inverter and the coincidence counts was measured for various delays. A graph was plotted and the region of maximum coincidence was obtained. With the aid of the provided curve fit, the center was found at around 23.65$\pm$ 0.19ns and FWHM of 28.3$\pm$ 0.61ns, so a delay of 23ns was used for the experiment.

The width of the plateau represents that the coincidence is happening well. Looking at the profile of the distribution, it was concluded that the delay of 23ns and the resolving time of 20ns was reasonable.

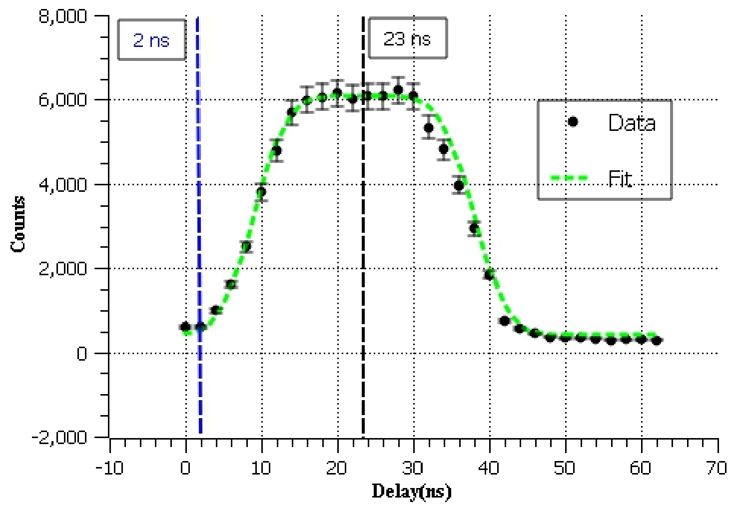

Figure 9: prompt curve

5.1.5 Setting up the slow coincidence

For the UC to give an output signal, the signals from the SCAs and the FC must be coinciding in time. This was done by connecting the outputs of the SCAs and the FC to an oscilloscope, and by changing the internal delays of the SCAs such that the signals coincided with the FC signal. The alignment was made by aligning the leading edges of the pulses.

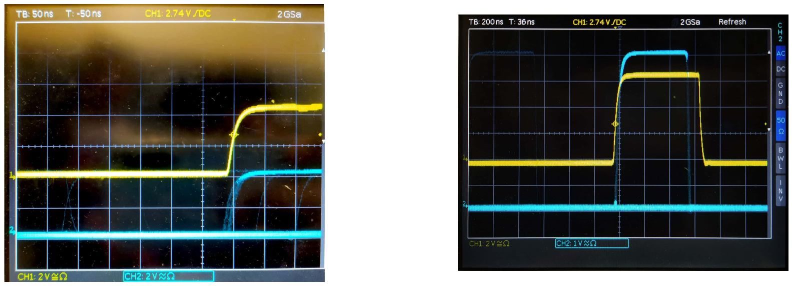

(a) Channel 1

(b) Channel 2

Figure 10: Setting up slow coincidence

5.1.6 Calibrating the SCAs

The SCAs were used to select γ ray events of the energy range corresponding to ^{60}Co transition. This was done by operating the SCAs in the window mode and selecting a window width of 20 channels. . The window width was kept constant all throughout the experiment because changing window widths would give varying counts and hence we cannot use the data for calibration. Using the graph, the window for the both the SCAs was set from channel 500 to 800 as both peaks were visible in this range.(Ref Figure 11).
With a window range of 20ns, it was possible to resolve the photopeaks well enough in order to choose a range of gamma rays, and still be able to take enough measurements within the short time we had (as we had to finish the experiment within 8 hours). Hence the setting was quite appropriate for gathering all the required information as we have quite a clear spectrum.
In addition we find that our measured gamma peaks and Compton edges almost match and select the channel range between 500-800 for both the SCAs.

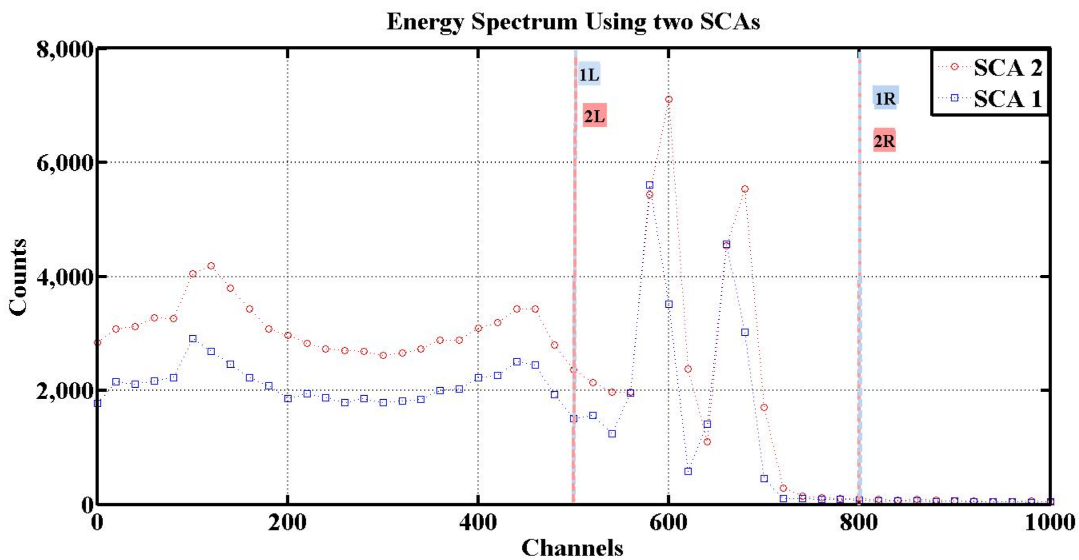

Figure 11: Energy spectrum obtained using the two SCAs. The two gamma ray peaks and Compton edge is clearly visible for both the graphs.The gamma ray peaks lie within the selected window range n_L to n_R for SCA_n, where n=1,2.

5.2 Main Measurement

5.2.1 Measurement of Angular Correlation

To measure the angular correlation, two types of measurements were made:

1. One set of measurements were made with fine stepping of 30°from 90°to 270°with a short count duration of 200±1s. This gives an idea of the overall angular dependence.

2. A second set of measurements were made at 90°, 135°, 165°, 180°, 195°, 225°, 235°with a longer count duration of 400±1s. These data help us to precisely predict the correlation coefficients. At least four readings were necessary to obtain the three unknown parameters A,B and C with an error bar associated with the fit.

5.2.2 Measurement of stability of setup

Readings were taken at 180°at three different time intervals:

1. At the beginning of the measurements.

2. In the middle of other measurements.

3. At the end of the measurements.

The count duration of each measurement was 400±1s. This was done to check the stability of the setup over the entire duration of the measurement process.

5.2.3 Measurement of random coincidence

The measured coincidence count includes true coincidences from the source, and random coincidences from various other sources such as less probable decay schemes, background radiation, etc. Random coincidences do have an angular correlation in the pressence of misalignment. But in absence of misalignment they don't have an angular correlation since the random sources of gamma rays causing the coincidence are isotropic in the Universe. For this measurement, the delay in the fast circuit was set at 2ns such that no true coincidence would be detected, ref Fig.9 and the counts were measured for a duration of 400s. The same reading was scaled for 200±1s.
Does an error arise from not changing the delay in the slow circuit? Since the random coincidences are background events which are not related to the source, changing the delay in the slow circuit will not have any effect on it.

6 Analysing the data

6.1 Subtracting random coincidence

A random coincidence count N_{random}=745 was obtained for a count duration of 400s at 180°with the fast delay time set to 12ns.We can use the same value of random coincidence for all angles because random coincidences do not have any angular correlation. Hence on subtraction from the coincidence count from the universal counter, gives the true count. N_{true}=N_{UC}-N_{random} for the measurements made for 400s.

Angle(°)	$N_{C1}(10^2)$	$N_{C2}(10^2)$	N_{UC}	N_{true}	Error
90	36738	38738	16171	15426	124.201449
135	36705	39292	16982	16237	127.424487
165	36806	39608	18262	17517	132.351803
180	36784	40010	18580	17835	133.547744
195	36750	40112	18262	17517	132.351803
235	36824	39810	16958	16213	127.330279
270	36718	39718	16577	15832	125.825277

Table 1:Angular correlation coincidence counts (measured for 400±1s each). N_{Cm} denotes the counts obtained by Counter-m, where m=1,2, N_{UC} is the coincidence counts from universal counter and N_{true}=N_{UC}-N_{random} with N_{random} = 745. The error is estimated using Poisson distribution($\sqrt{N_{true}}$)

6.2 Fitting a curve to the obtained data

- The true coincidence data obtained is fitted using the method least squares with

$$W(\theta) = W_0(1 + A_{22}(Q_{22})^2 cos^2(\theta) + A_{44}(Q_{44})^2 cos^4(\theta)$$

  where W_0 is the scaling factor to the theoretical formula Q_2=0.9057 and Q_4=0.7114 are the solid angle corrections obtained for 2"×2" crystal.

- **Fit 1: Fitting the curve to the data taken at various angles for 200±1s.** The curve is fitted to all true coincidences data points as mentioned in table 2. It has been observed that the fitted curve does deviate from the theoretical at a lot of points to some extent. From this, we obtain A_{22}=0.147±0.0075 and A_{44}=0.0143±0.0583.

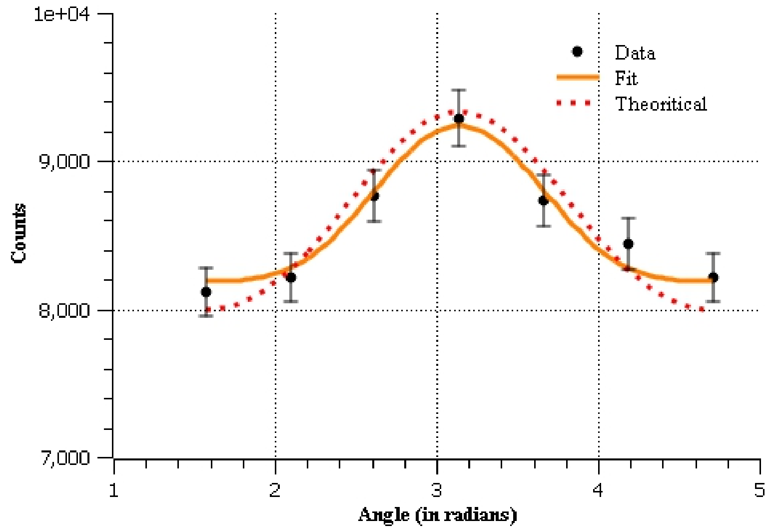

Figure 12: Fit 1: Curve fit to the coincidence counts for 200±1s

- **Fit 2: Fitting the curve to the data taken at various angles for 400±1s.** From this, we obtain A_{22}=0.112±0.0104 and A_{44}=0.0522±0.009

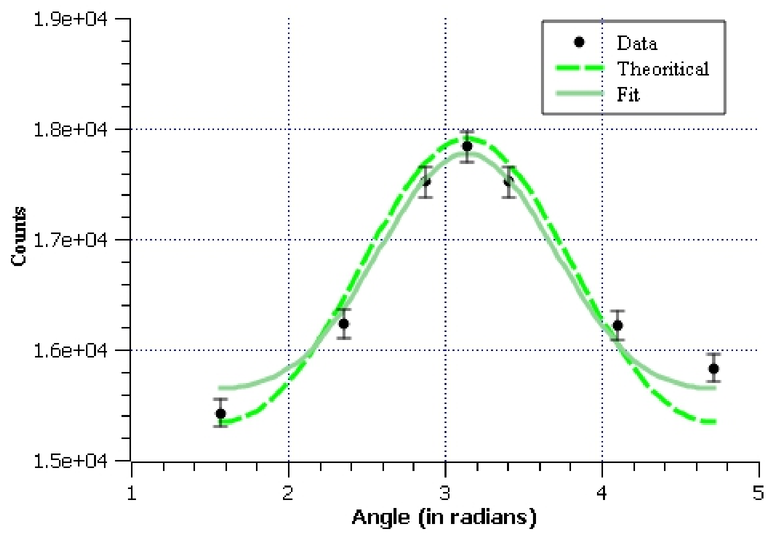

Figure 13: Fit 2: Curve fit to the coincidence counts for 400±1s

The black error bars denote the Poisson errors for counts and $\pm 1^\circ$for angle.

6.3 Fitting angular correlation functions for cascades with other spins

To remove the possibility of other decay schemes, a fitting for the 0-2-0 cascade was also done.

$$W(\theta) = W_0(1 + A_{22}(Q_2)^2 cos^2(\theta) + A_{44}(Q_4)^2 cos^4(\theta))$$

with A_{22}=0.3571, A_{44}=1.143 being the theoretically predicted coefficients of the 0-2-0 cascade and Q_2=0.9057, Q_4=0.7114 are the solid angle corrections. The parameters W_0 was varied to obtain the best fit. The fitted curve is shown in Figure 14. The values of A_{22} and A_{44} for the 0-2-0 cascade prediction was found to be 0.237±0.0062 and 0.0089±0.0461 respectively with χ^2=16.5. On the other hand we find A_{22} and A_{44} to be respectively 0.147±0.0075 and 0.0143±0.0583 which are much closer to the theoretically predicted values of 0.125 and 0.042 respectively. Hence, we can conclude that, A_{22} and A_{44} obtained values fit better to the prediction of 4-2-0 cascade. Hence we can exclude the possibility of 0-2-0 cascade.

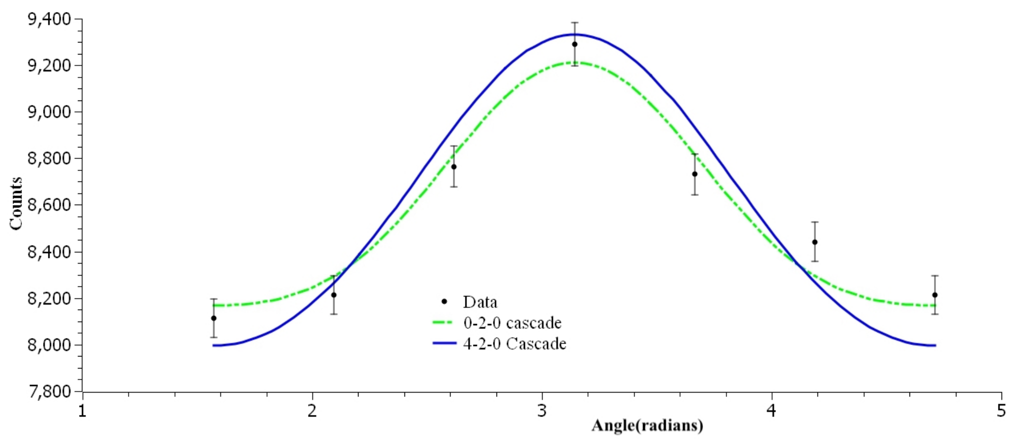

Figure 14: The angular correlation function for 0-2-0 cascade was fitted to the coincidence data obtained for 200±1s. The theoretically predicted graph for the 4-2-0 cascade is also plotted for comparison.

6.4 Stability of the system

Measurements of coincidence counts was taken at three different times at 180°, as mentioned in section 5.2.2. The stability of the system is not clear from our plot. This is because we don't have enough data points to conclude something completely. At the first glance we see that there is an observable difference between the counts for the first two measurements (one at the beginning and another after 25 minutes). However, the count number at the end of the measurement was more or less similar to the count number at 25 min. A rough estimate of the error is found to be ($\sim$250). Hence we see that systematic error is less than the statistical error thus our system seems less unstable but then again we cannot conclude for sure because we don't have enough data measurements.

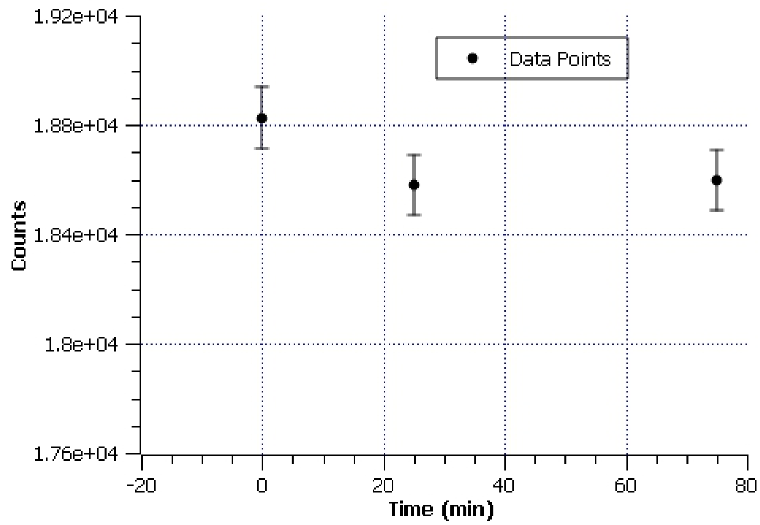

Figure 15: Coincidence count obtained for 400s at 180°at different times.

7 Results

- The coefficients obtained by curve fitting are summarized in Table 2. The obtained coefficients deviate from the theoretical values (A_{22}=0.125 and A_{44}=0.042) to some extent. The fitted curves deviates from the theoretical at the extrema. From Fit 1 and Fit 2, obtained results can be explained if time dependent systematic errors are taken into consideration.

	Fit 1 (200±1s)	Fit 2 (400±1s)
W_0	8188.45 ± 77.51	8188.45 ± 77.5216
A_{22}	0.147 ± 0.0075	0.112 ± 0.0104
A_{44}	0.0143 ± 0.0583	0.0522 ± 0.0090
χ^2	4.5	NA

Table 2: Coefficients and χ^2 obtained for the fits.

- The system is unstable over time but cannot be said with certainity as we have taken only 3 data measurements out of which two data sets are close to each other as shown in Fig.15 . This time dependence cannot be attributed to the room temperature and cannot be explained by the Poisson error distribution. The possible cause for the error could be because of the efficiency and stability of the electrical components like the amplifiers and detectors with time.

- When the data was fitted to the angular correlation function of the cascade with spin 0-2-0, we found that χ^2=16.5 which is much higher than the χ^2=4.5 obtained for the cascade with spin 4-2-0. Thus, 0-2-0 cascade can be excluded.

8 Conclusion

A detector setup was used to measure the γ-γ angular correlation in the decay of ^{60}Co. Before taking measurements, the energy and timing branches were adjusted by adjusting the amplifier gain and threshold of the Constant-Fraction-Discriminator. The Fast and Slow coincidence circuits were calibrated along with the Single Channel Analysers. The coincidence counts were recorded for various angles for measuring the angular correlation It is seen that the obtained value of the correlation coefficients deviates but is close to the theoretically predicted 4-2-0 spin cascade for ^{60}Co.

9 Appendix

Angle($^{\circ}$)	N_{UC}	N_{true}	$N_1(10^2)$	$N_2(10^2)$	Error
90	8113	7368	18344	19344	85.8324
120	8214	7469	18387	19433	86.4276
150	8764	8019	18378	19779	89.5412
180	9289	8544	18367	19980	92.4319
210	8732	7987	18350	20031	89.3765
240	8441	7696	18387	19880	87.7255
270	8212	7467	18334	19834	86.4106

Table 3: Coincidence counts measured for 200±1s each. Here, $N_{true} = N_{UC} - N_{random}$ with $N_{random} = 745$. Error=$\sqrt{N_{true}}$.

Time(min)	N_{UC}	N_{true}
0	18826	18081
25	18581	17836
74	18598	17853

Table 4: Coincidence counts measured for 400±1s at 180°, at different times of the experiment.

References

[1] *University of Bonn: Instructions of K223 – Nuclear γ-γ Angular Correlations.* State: February 2020.

[2] *R.B. Firestone, Table of Isotopes 8th edition.* Wiley, New York(1996).

[3] *K. Siegbahn, ALPHA-, BETA- AND GAMMA-RAY SPECTROSCOPY.* Vol.2, North Holland Publishing Company, Amsterdam(1965)

[4] *Canbera Elecktronik, Constant Fraction Discriminator Model 1326, 1428 Operating Manual.* Digital copy, accessed in February 2020.

[5] *Ametek Ortec, Single Channel Analysers.* Digital copy, accessed in February 2020.

[6] *Ametek Ortec, Fast Coicidence 414A Brochure.* Digital copy, accessed in February 2020.

[7] *Ametek Ortec, Universal Coicidence 418A Brochure.* Digital copy, accessed in February 2020.

[8] *Ametek Ortec, Educational experiments.* Digital copy, accessed in February 2020.